**The EMBO Journal** Vol.18 No.17 pp.4856–4864, 1999

# A conformational switch at the 3′ end of a plant virus RNA regulates viral replication

**René C.L.Olsthoorn, Sander Mertens, Frans T.Brederode and John F.Bol[1]**

Institute of Molecular Plant Sciences, Gorlaeus Laboratories, Leiden University, PO Box 9502, 2300 RA Leiden, The Netherlands

[1]Corresponding author
e-mail: J.bol@chem.leidenuniv.nl

**3′ untranslated regions of alfamo- and ilar-virus RNAs fold into a series of stem–loop structures to which the coat protein binds with high affinity. This binding plays a role in initiation of infection ('genome activation') and has been thought to substitute for a tRNA-like structure that is found at the 3′ termini of related plant viruses. We propose the existence of an alternative conformation of the 3′ ends of alfamo- and ilar-virus RNAs, including a pseudoknot. Based on (i) phylogenetic comparisons, (ii) *in vivo* and *in vitro* functional analyses of mutants in which the pseudoknot has been disrupted or restored by compensatory mutations, (iii) competition experiments between coat protein and viral replicase, and (iv) investigation of the effect of magnesium, we demonstrate that this pseudoknot is required for replication of alfalfa mosaic virus. This conformation resembles the tRNA-like structure of the related bromo- and cucumo-viruses. A low but specific interaction with yeast CCA-adding enzyme was found. The existence of two mutually exclusive conformations for the 3′ termini of alfamo- and ilar-virus RNAs could enable the virus to switch from translation to replication and vice versa. The role of coat protein in this modulation and in genome activation is discussed.**

*Keywords*: alfalfa mosaic virus/conformational switch/pseudoknot/tRNA-like structure/viral replication

## Introduction

The 3′ termini of the genomic RNAs of many positive-strand RNA viruses of plants possess a tRNA-like structure (TLS) which is recognized by tRNA-specific enzymes (Mans *et al.*, 1991; Giegé, 1996; Haenni and Chapeville, 1997). Plant viruses with a 3′ TLS include members of the tymo-, tobamo-, tobra-, bromo-, cucumo-, hordei- and furo-viruses (Goodwin and Dreher, 1998). A crucial step in obtaining tRNA mimicry is the formation of a so-called pseudoknot: an RNA hairpin in which loop residues base pair with nucleotides outside that loop (Pleij, 1994). Inherent to pseudoknots is their low stability which often results in the folding of alternative structures (Wyatt *et al.*, 1990; Gluick *et al.*, 1997; Kolk *et al.*, 1998). This property allows pseudoknots to function as 'molecular switches', e.g. in regulating translation of the alpha and repZ mRNA (Draper, 1996; Asano and Mizobuchi, 1998). The role of the pseudoknot in the TLS of plant viral RNAs is quite puzzling. On one hand, the pseudoknot as a central part of the TLS is required for aminoacylation of bromo- and tymo-viruses (Dreher and Hall, 1988; Mans *et al.*, 1992) but then aminoacylation itself is not mandatory for virus accumulation in plants (Dreher *et al.*, 1989; Goodwin *et al.*, 1997). On the other hand, several experiments indicate that the pseudoknot is dispensable for replication *in vitro* (Deiman *et al.*, 1998; Singh and Dreher, 1998; Chapman and Kao, 1999), whereas it remains essential for replication of these viruses *in vivo* and cannot be replaced by a genuine tRNA (Skuzeski *et al.*, 1996). Such data are suggestive of a possible regulatory role for the pseudoknot in the TLS of plant virus RNAs.

The family of Bromoviridae contains several genera of plant viruses with a tripartite RNA genome. Within this family, bromo- and cucumo-viruses possess a TLS that can be charged with tyrosine, whereas the RNAs of alfalfa mosaic virus (AMV; the type member of the alfamoviruses) and ilarviruses cannot be charged with an amino acid, and are believed to lack a TLS. Instead, the 3′ termini of the RNAs of AMV and ilarviruses contain a site that binds viral coat protein (CP) with high affinity, and binding of CP to the inoculum RNAs is required to initiate infection (reviewed in Bol, 1999; Jaspars, 1999). The function of CP in the inoculum has been termed 'genome activation'. It has been suggested that CP binding functionally compensates for the absence of a TLS (Neeleman *et al.*, 1993; Houser-Scott *et al.*, 1997).

The 3′ untranslated regions (UTRs) of the AMV genomic RNAs share a terminal sequence of 145 bases that can be folded into a linear array of stem–loop structures, as first proposed in 1979 (Koper-Zwarthoff *et al.*, 1979) (Figure 1, top). The secondary structure of this region has been verified by phylogenetic comparison and enzymatic structure mapping (Koper-Zwarthoff and Bol, 1980; Houwing and Jaspars, 1982; Quigley *et al.*, 1984). The 3′ UTRs have been shown to contain multiple high-affinity binding sites for CP, which are characterized by hairpins flanked by AUGC motifs (Bol, 1999). In particular, the integrity of the terminal hairpin (Figure 1, top), which is strongly conserved in AMV and ilarviruses, is an important parameter for CP binding (Reusken and Bol, 1996; Ansel-McKinney and Gehrke, 1998).

Here we show that the 3′ terminus of AMV and ilarvirus RNAs can adopt an alternative conformation through the formation of a pseudoknot. The pseudoknot conformation resembles the TLS of bromo-, cucumo- and hordei-viruses and a weak, though specific, interaction of the AMV 3′ UTR with the CCA-adding enzyme from yeast was found. By mutation analysis of the AMV 3′ end we demonstrate that this pseudoknot is essential for viral replication *in vivo* and *in vitro*. We also show that binding of CP to the 3′ end inhibits production of minus-strand

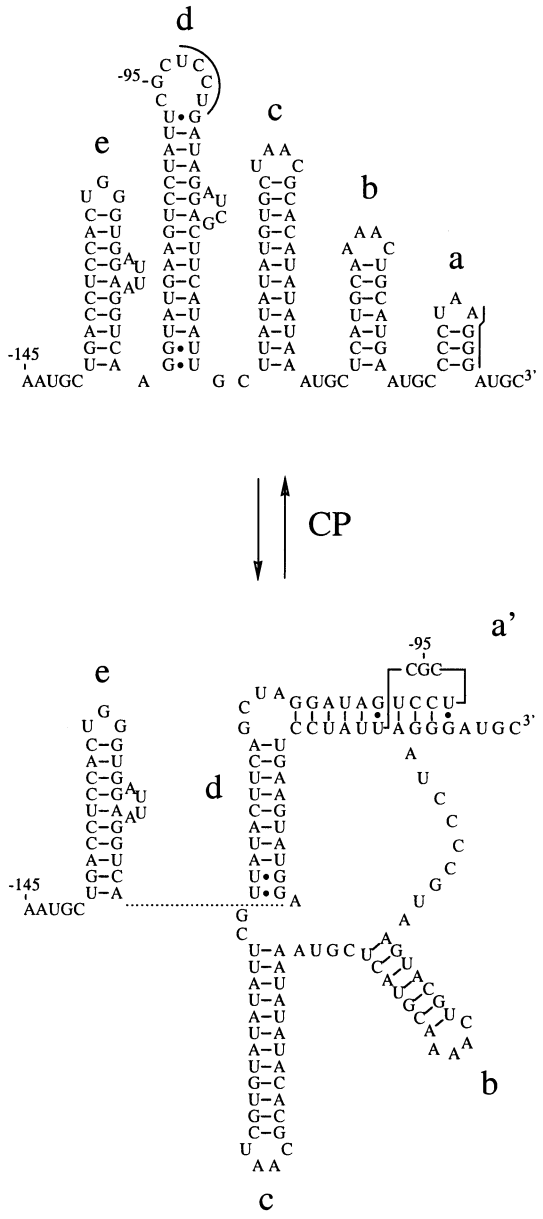


**Fig. 1.** Two mutually exclusive conformations of the terminal 145 nt of the 3′ UTR of AMV RNA3. Top: the well known CP-binding structure. Bottom: pseudoknotted structure formed upon pairing of the overlined sequences in the top figure. The dotted line represents a single phosphodiester bond between two nucleotides. Hairpins are indicated by lower case (a–e), the pseudoknot by a'. The influence of CP on the two conformations is discussed in the text.

RNA by interfering with the formation of the pseudoknot. The 3′ terminus of AMV and ilarvirus RNAs thus has a dual role in the life cycle of these viruses: one for the production of minus strands, the other for the binding of CP. We propose that binding of CP to the inoculum RNAs of AMV and ilarviruses plays a role in translation of these RNAs or in other steps of the replication cycle that precede the initiation of RNA replication. Later in the infection process, binding of newly synthesized CP to the 3′ end of plus-strand RNAs may shut off minus-strand synthesis, thereby triggering a switch to the asymmetric synthesis of plus-strand viral RNAs.

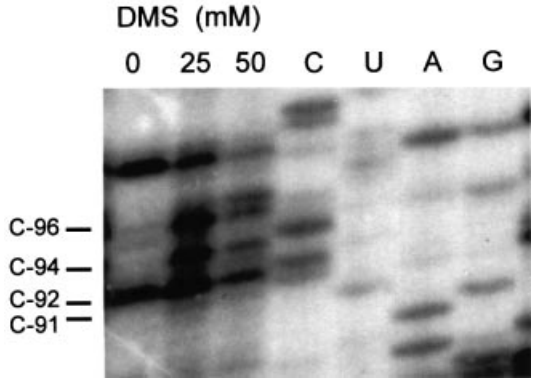


**Fig. 2.** Sensitivity of nucleotides in loop d of RNA4 to modification by DMS. Left three lanes, RNA4 was incubated with the indicated amount of DMS at room temperature for 30 min. After purification, the modified bases were detected by primer extension with a primer complementary to the terminal 21 nucleotides. Right four lanes, RNA sequence obtained by primer extension on RNA4 in the presence of dideoxynucleotides. The latter lanes are shifted one nucleotide up with respect to the DMS lanes due to the fact that reverse transcriptase stops elongating at a modified base but terminates after addition of a dideoxynucleotide.

## Results

### *Biochemical and phylogenetic data in support of the existence of an alternative structure within the 3′ end of AMV and ilarvirus RNAs*

The secondary structure of the 3′ UTR of AMV genomic RNAs is usually depicted as a linear array of stem–loop structures, flanked by AUGC motifs (Figure 1, top). We believe that an alternative conformation exists (Figure 1, bottom) that is mutually exclusive with the CP-binding conformer. This alternative structure is formed when nucleotides UCCU in loop d base pair with residues AGGG in stem a, resulting in a pseudoknot. This conformation is still in agreement with structure-probing data that showed reactivity of bases in loop d and stem a to both single- and double-strand-specific enzymes (Quigley *et al.*, 1984). Moreover, nucleotides that are crossing the major groove of a pseudoknot, here CGC, are relatively inaccessible to nucleases (van Belkum *et al.*, 1985). The low reactivity of G-95 (numbering starts at the 3′ end) towards RNase T1 (Houwing and Jaspars, 1982) is therefore in good agreement with a pseudoknotted conformation. In our hands, probing with dimethyl sulfate (DMS), which reacts with N3 of unpaired cytosines, showed that both C-94 and C-96 are readily modified in contrast to C-91 and C-92 (Figure 2), which are predicted to be base-paired in the pseudoknot conformation. We note that C-92 coincides with a non-specific stop in the primer extension reaction but nevertheless its intensity is not enhanced by DMS treatment.

The pseudoknot interaction is also supported by phylogenetic data. As illustrated by Figure 3, similar pseudoknot structures can be folded in the RNAs of all known ilarviruses. In several RNAs it is possible to extend base pairing towards the 3′ end. We note that in AMV RNA the interaction can also be drawn such that a terminus with three instead of four unpaired nucleotides results. At present we cannot discriminate between these two possibilities. Since it is difficult to predict the loop sizes in a pseudoknot we have drawn all RNAs with an unpaired

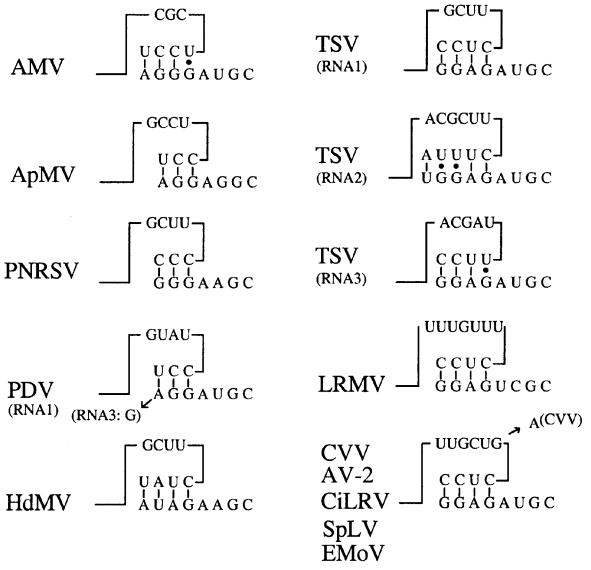


**Fig. 3.** Conservation of the pseudoknot in all other ilarvirus RNAs. AMV, RNAs 1, 2 and 3 of all known isolates; PDV, prune dwarf virus RNAs 1 and 3; PNRSV, *Prunus* necrotic ringspot virus (three strains) RNA3; ApMV, apple mosaic virus (two strains) RNA3; HdMV, hydrangea mosaic virus RNA3; TSV, tobacco streak virus RNAs 1, 2 and 3; LRMV, lilac ring mottle virus RNA3; CVV, citrus variegation virus RNA3; CiLRV, citrus leaf rugose virus RNAs 1, 2 and 3; EMoV, elm mottle virus RNAs 1, 2 and 3; AV-2, asparagus virus 2 RNA3; and SpLV, spinach latent virus RNAs 1, 2 and 3.

terminus of four bases. Sequence comparison also revealed that the 3′ UTR of ilarvirus RNAs can exist in two mutually exclusive conformations (data not shown).

### *Similarities of the AMV pseudoknot conformation with the TLS of other Bromoviridae and its interaction with the CCA-adding enzyme*

The pseudoknotted conformer of AMV RNA (and of ilarvirus RNAs) shows similarities with the pseudoknot structures present at the 3′ end of bromo-, cucumo- and hordei-virus RNAs (Figure 4), which all possess tRNA-like features. The 3′ UTR of the genomic RNAs of olive latent virus 2 (OLV-2), the type species of the genus *Oleavirus*, can be readily folded into a TLS in our hands (Figure 4), in contrast to earlier reports (Grieco *et al.*, 1996). The resemblance of the AMV pseudoknot structure with these TLSs and the fact that alfamo-, ilar-, bromo-, cucumo- and olea-viruses are all members of the same family, the Bromoviridae, prompted us to re-investigate putative tRNA-like features of AMV RNA.

Attempts to aminoacylate AMV RNA have been unsuccessful so far (Hall, 1979; R.C.L.Olsthoorn and J.F.Bol, unpublished data), possibly due to the lack of a CCA terminus. Therefore we tested whether the 3′ UTR of AMV RNA3 was a substrate for CTP/ATP:tRNA nucleotidyl transferase. This enzyme is responsible for the addition of CCA ends to tRNAs and to various plant viral RNAs (Mans *et al.*, 1991), and is sensitive to the length of the aminoacyl-acceptor (aa) arm, which should be ~11–13 bp (Shi *et al*., 1998). In AMV RNA a putative aa arm of 11 bp can be formed by extending the horizontal helix with a U–A pair such that the connecting loop becomes UCGA instead of AUCG (Figure 4). This loop could be the equivalent of the T-loop in tRNA and in a way resembles the connecting loop in the TLS of BSMV (Figure 4).

A synthetic transcript corresponding to the 180 nt-long 3′ UTR of AMV RNA3 could be labelled with [$^{32}$P]AMP by the CCA-adding enzyme from yeast (Figure 5, WT). Labelling also took place in the absence of CTP (data not shown), suggesting that the AUGC terminus is extended by a single adenosine. This reaction was strongly dependent on the presence of $Mn^{2+}$; however, under these conditions adenylation was still specific, as a fragment lacking the terminal 90 nt was not labelled (Figure 5, DR). In the absence of $Mn^{2+}$, labelling was estimated to be 50-fold less efficient than adenylation of a synthetic tRNA-CC transcript (data not shown).

To show that adenylation of AMV RNA was specific for the presence of the putative aa arm, mutations were made in the pseudoknot (Figure 6). Mutants with a disrupted pseudoknot, G3, C3 and A4, showed a reduced level of adenylation (Figure 5). In contrast, when the pseudoknot was restored by compensatory mutations, a wild-type (wt) level of adenylation was again observed (Figure 5, GC3). Although the biological significance of this type of labelling needs further investigation, these data do support the presence of a quasi-continuous helix of 11–13 bp at the 3′ terminus of AMV RNA.

### *Role of the pseudoknot in viral replication*

To examine the function of the pseudoknot in viral replication, pseudoknot mutations were introduced into full-length RNA3 transcripts, which were inoculated onto P12 tobacco plants. These plants are transgenic for the P1 and P2 replicase genes encoded by AMV RNAs 1 and 2, respectively. AMV RNA3 encodes the viral movement protein (P3) and the CP, which is translated from the subgenomic RNA4. Infection with RNA3 of P12 plants results in the accumulation of viral particles containing either RNA3 or subgenomic RNA4 (Taschner *et al.*, 1991). Figure 7A shows that the possibility of forming the pseudoknot also correlated well with the accumulation of viral RNAs. Mutants C2, G3 and C3 (Figure 6), in which 2 or 3 bp in the pseudoknot are disrupted, did not accumulate to detectable levels, in contrast to mutants GC2 and GC3 in which the pseudoknot interaction is restored (Figure 7A). In P12 protoplasts, essentially the same results were obtained (Figure 7B). The accumulation of mutant A4 both in plants and protoplasts never exceeded 10% of the wt level (data not shown).

The role of the pseudoknot in recognition of the AMV RNAs by the viral RNA-dependent RNA polymerase (RdRp) was analysed by using wt and mutant RNAs as templates for the purified AMV RdRp in an *in vitro* assay (de Graaff *et al.*, 1995). Figure 7C shows that template activity of the mutant RNAs *in vitro* paralleled their accumulation *in vivo* (Figure 7A and B), suggesting that a reduced accumulation *in vivo* is mainly due to a defect in minus-strand synthesis.

### *CP inhibits minus-strand synthesis by untying the pseudoknot*

From the above experiments it is clear that the pseudoknot conformation is required for minus-strand synthesis. On the other hand, the ‘linear conformation’ (Figure 1, top) has been implicated in CP binding. Studies on thermal melting profiles (Hinz *et al.*, 1979), ethidium bromide binding (Srinivasan and Jaspars, 1982), circular dichroism

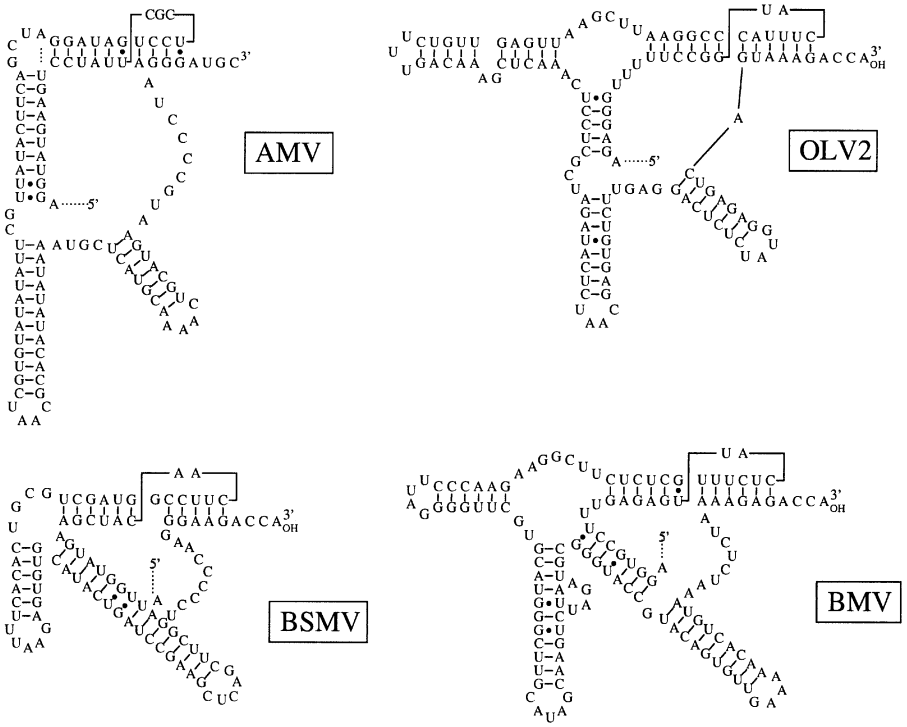


**Fig. 4.** Structural similarity of the pseudoknotted conformation of AMV with the tRNA-like structures present at the 3′ end of some related plant viral RNAs. BMV, brome mosaic bromovirus, the structure according to Rietveld *et al.* (1983) is shown; BSMV, barley stripe mosaic hordeivirus, according to Kozlov *et al.* (1984); OLV-2, olive latent oleavirus (Grieco *et al.*, 1996), putative folding. Cucumoviruses resemble BSMV in their TLSs. An alternative U–A base pair that extends the quasi-continuous helix in AMV to 11 bp is indicated by a dotted line.

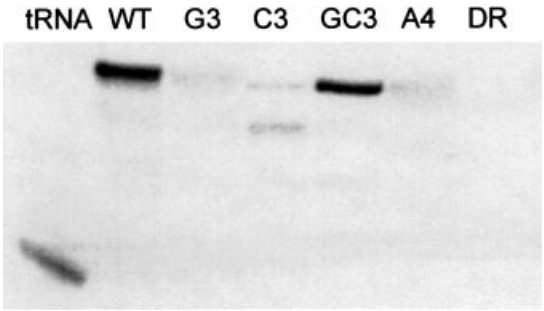


**Fig. 5.** Adenylation of AMV 3′ UTR by CTP/ATP:tRNA nucleotidyl transferase from yeast. Transcripts of 180 nt corresponding to wt or mutant 3′ UTR of RNA3 were incubated with yeast transferase and [$^{32}$P]ATP for 2 h at room temperature in a buffer containing both $Mg^{2+}$ and $Mn^{2+}$. Mutants G3, C3, GC3 and A4 are depicted in Figure 6. DR is a transcript that lacks the terminal 90 nt of AMV RNA3. Yeast tRNA from which the terminal A had not been removed served as a control.

(Srinivasan and Jaspars, 1982; Baer *et al.*, 1994), electrophoretic mobility in native gels (Baer *et al.*, 1994) and RNase protection (Houwing and Jaspars, 1982) indicated that binding of CP causes a conformational change in the 3′ UTR. In the light of our present data, CP binding presumably induces a transition from the pseudoknot conformer to the CP-binding conformer, which is not recognized by the RdRp. Such a scenario would fit with the observation that addition of CP to the *in vitro* RdRp assay blocks minus-strand synthesis (de Graaff *et al.*, 1995). From this scenario it also follows that replication of a mutant in which such a switch cannot occur would not be affected by the addition of CP. To examine this possibility, the template activities of wt RNA and mutant 1-7 in the RdRp assay were compared in the absence and presence of added CP. In mutant 1-7, stem–loop a is disrupted without disturbing the pseudoknot interaction (Figure 4). Previously, we have shown that this mutation interferes with binding of CP but has little effect on the template activity *in vitro* (Reusken *et al.*, 1997). The left panel of Figure 8 shows that addition of CP to CP:RNA ratios of 0.2 and 2, strongly inhibited template activity of wt RNA in the RdRp assay. In contrast, addition of CP did not affect the template activity of mutant 1-7 (Figure 8, right panel). These data support the hypothesis that binding of CP depends on formation of stem–loop a, thereby disrupting the pseudoknot required for RdRp recognition. Moreover, our data also indicate that the inhibitory effect of CP on minus-strand synthesis is due to binding of CP to the template RNA rather than binding to the RdRp.

### *$Mg^{2+}$ interferes with CP binding by stabilizing the pseudoknot conformation*

It is well documented that pseudoknots are stabilized by $Mg^{2+}$ (reviewed in Draper, 1996). It has also been reported that binding of CP to the 3′ end of AMV RNA1 but not to internal sites was inhibited by $Mg^{2+}$ (Zuidema, 1983). We hypothesized that addition of $Mg^{2+}$ would favour the formation of the pseudoknot, which in turn would preclude CP binding. To test this hypothesis, we performed band shift assays with a transcript comprising the terminal 112 nt of AMV RNA3, i.e. the 'L-shape' formed by elements a', b, c and d (Figure 1, bottom). In the absence of $Mg^{2+}$, addition of CP to the wt transcript resulted in a clear shift (Figure 9, D/WT). In the presence of 10 mM $Mg^{2+}$, however, CP was hardly capable of forming a complex (Figure 9, D/WT). In contrast, $Mg^{2+}$ did not

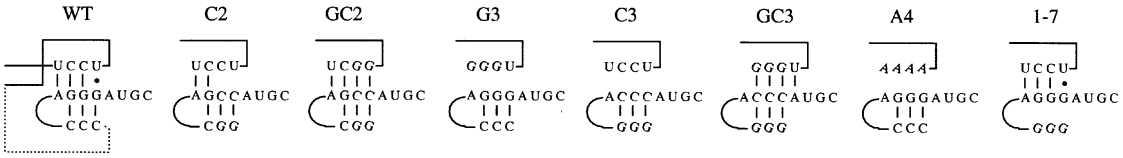


**Fig. 6.** Pseudoknot mutants used in this study. Mutated bases are printed in italics. Dashes between nts indicate possible base pairings. Note that, except for mutant 1–7, all mutants have the potential to form hairpin a and only differ in their ability to form the pseudoknot structure.

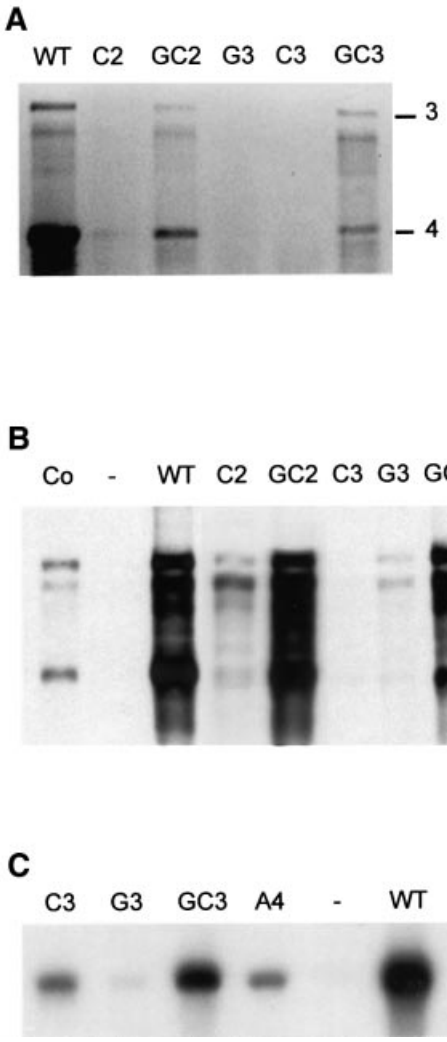


**Fig. 7.** (**A**) Accumulation of virion RNAs 3 and 4 in P12 tobacco plants inoculated with wt and mutant RNA3 transcripts. Purified RNA was electrophoresed in an EtBr-containing agarose gel (1.4%) and visualized under UV (a reverse print is shown). (**B**) Northern blot showing the accumulation of wt and mutant RNAs in P12 tobacco protoplasts; Co, RNA3 and RNA4 markers; (–), mock-inoculated sample. (**C**) Autoradiogram of products synthesized by *in vitro* replication on wt and mutant RNA3 using purified AMV RdRp. (–), no template was added to the reaction. The template activities of C2 and GC2 were similar to those of C3 and GC3, respectively.

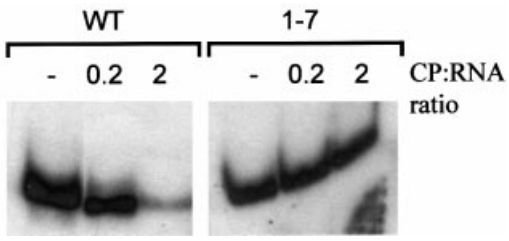


**Fig. 8.** *In vitro* RdRp assay in the absence (–) or presence of added CP (0.2–2 mol CP/mol RNA). RNA templates were pre-incubated with CP before the addition of purified AMV RdRp. WT, wild-type transcript corresponding to the 3′ UTR of AMV RNA3 was used as template; 1-7, like WT but containing mutations as shown in Figure 6. We note that the template activity of mutant 1-7 is 50–85% that of wt (Reusken *et al.*, 1997; R.C.L.Olsthoorn and J.F.Bol, unpublished results), possibly because it can also form an alternative pseudoknot involving the three G residues at positions 11, 12 and 13 from the 3′ end (Figure 6).

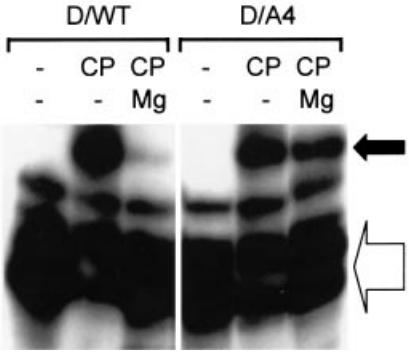


**Fig. 9.** Band shift assay with CP in the absence or presence of $Mg^{2+}$. $^{32}$P-labelled transcripts (~20 pmol) were renatured in the absence or presence of $Mg^{2+}$ before the addition of CP (~5 pmol). Complexes were resolved on a 6% polyacrylamide gel. D/WT, a wt transcript comprising the terminal 112 nt of AMV RNA3 was used as probe; D/A4, a mutant transcript that cannot form the pseudoknot was used as probe. Big arrow, free probe; small arrow, RNA–CP complex.

severely inhibit CP binding to a mutant transcript that cannot form the pseudoknot (Figure 9, D/A4). These results show that it is the formation of the pseudoknot, and not the presence of $Mg^{2+}$ *per se*, which interferes with CP binding. Thus, under physiological conditions the equilibrium might well be in favour of the pseudoknot conformation, especially if host proteins can stabilize this structure.

## Discussion

We have shown here that the 3′ UTR of AMV and ilarvirus RNAs contains a pseudoknot structure that is required for viral replication. For the past 20 years, all research on the 3′ UTR of AMV and ilarvirus RNAs has been focused on an alternative structure that is involved in the binding of CP. Re-examination of the biochemical and phylogenetic data which were used to support the secondary structure of the CP-binding conformer led us to propose an alternative, pseudoknotted, conformer. Which of the two conformers is prevailing probably depends on experimental conditions such as temperature and (divalent) salt concentrations. Previously, enzymatic structure probing was carried out at either 37 (Quigley *et al.*, 1984) or 25°C (Houwing and Jaspars, 1982), whereas our chemical probing was performed at 21°C.

These different conditions could account for the 'alternate structures' observed by Quigley *et al.* (1984) but not by Houwing and Jaspars (1982) nor by us. In this respect it is worthwhile to note that thermal melting studies on AMV RNA4 showed a clear transition at 25.5°C (Srinivasan and Jaspars, 1978), which has been interpreted as the loss of tertiary structure. This transition was absent in a fragment consisting of the terminal 90 bases of RNA4 (Srinivasan and Jaspars, 1979), in other words, in a fragment that cannot form a stable pseudoknot. It is conceivable that under physiological conditions the genomic RNAs are predominantly in the pseudoknotted conformation and that CP binding shifts the equilibrium towards the linear conformation. This is further substantiated by the following observations. (i) Binding of CP to RNA4 coincides with the loss of the thermal transition at 25.5°C, pointing to '. . . an interference of the coat protein with the tertiary structure . . .' (Srinivasan and Jaspars, 1979). (ii) In native RNA4, position G-95 is not sensitive to RNase T1 digestion, probably due to steric hindrance in the pseudoknot conformation (van Belkum *et al.*, 1985). However, in nucleoprotein complexes of RNA4 and CP, G-95 is accessible for RNase T1 digestion (Houwing and Jaspars, 1982), indicating that G-95 is now part of the normal hairpin–loop d (Figure 1, top).

The conformational switch that is triggered by CP binding could have several functions in the viral life cycle. After dissociation of parental virus into RNA and CP, a few CP molecules probably remain associated to high-affinity binding sites at the 3′ termini of the inoculum RNAs. This CP may function in steps of the replication cycle that precede initiation of minus-strand RNA synthesis, such as protection of the 3′ end of viral mRNAs from exonucleolytic degradation (Neeleman *et al.*, 1993), enhancement of translation of viral mRNAs or prevention of a collision between translating ribosomes and replicase molecules synthesizing minus strands. Possibly, targeting of the parental RNAs to chloroplast membranes where replication complexes are assembled (de Graaff *et al.*, 1993) could result in the dissociation of the terminally bound CP, thereby permitting the formation of the pseudoknot structure and the initiation of minus-strand RNA synthesis.

Later in the infection process, newly synthesized CP will compete with the viral RdRp for binding to the 3′ end of plus-strand RNAs. Since CP is made in large excess over the P1 and P2 replicase subunits, the pseudoknot conformation will eventually collapse and minus-strand synthesis be shut off. This will then be the trigger to commence with the asymmetric synthesis of plus-strand viral RNAs. This view fits well with the role of CP in asymmetric plus-strand RNA synthesis observed *in vivo* (Bol, 1999).

So far, there is no experimental evidence to support an early function of CP in the translation of inoculum RNAs. The 3′ UTRs of several plant viral RNAs are known to be involved in the initiation of translation (Lahser *et al.*, 1993; Leathers *et al.*, 1993). Also, the 3′ UTR of AMV RNA4 has been shown to stimulate translation *in vitro* and in oocytes, but this stimulation was reported to be independent of CP (Ryabova *et al.*, 1993; Hann *et al.*, 1997). However, this does not exclude a role of CP in the translation of AMV RNAs 1 and 2 *in vivo* when viral replicase is expressed. Moreover, it might be interesting to study the effect of CP on translation of RNAs 1 and 2 *in vitro* in the presence of purified AMV RdRp.

The pseudoknot structure of AMV (and ilarviruses) shows similarities with the TLS of bromo- and cucumoviruses, which are also members of the family of Bromoviridae. Recently, OLV-2 has been included as a member of this family (Pringle, 1998). The 3′ UTR of the three genomic RNAs of this virus can also be folded into a TLS (Figure 4). It is therefore tempting to speculate that all members of the family of Bromoviridae possess a TLS but that AMV and ilarviruses have evolved a divergent version to accommodate CP binding. Thus, the members of this family may be more related than previously realized. This latter assumption is corroborated by the observation that the brome mosaic virus (BMV) RdRp prefers to initiate replication on AUGC over ACCA termini (Deiman, 1999).

The TLS of bromo- and cucumo-viruses possesses tRNA-specific functions such as being a substrate for the CCA-adding enzyme and tyrosyl-tRNA synthetase. The TLS of BMV RNA contains additional charging capacities for valine and histidine (Felden *et al.*, 1998). No data are available for OLV-2, but considering the resemblance with BMV, charging with tyrosine, valine or histidine is predicted. Attempts to charge AMV RNAs have not been successful so far (Hall, 1979; R.C.L.Olsthoorn and J.F.Bol, unpublished data). On one hand this may be due to the lack of a CCA end; on the other hand, not all plant viruses possessing a TLS are capable of aminoacylation. Notorious exceptions are tomato aspermy cucumovirus, tobraviruses and some furoviruses (Mans *et al.*, 1991; Goodwin and Dreher, 1998). Yet tRNA-specific enzymes could still play a role in the life cycle of these viruses. Possibly, AMV and ilarviruses can also interact with an aminoacyl tRNA synthetase without becoming aminoacylated. Currently, we are investigating whether addition of AMV RNA has an adverse affect on tRNA aminoacylation.

As a hint to a possible TLS in AMV, we found a weak adenylation by the yeast CCA-adding enzyme. Although this reaction was strongly dependent on the addition of $Mn^{2+}$, which is not very common for this enzyme, it was specific for the presence of the pseudoknot structure. We found that $Mn^{2+}$ was also needed to restore adenylation of tRNA–UGC to the same level as that of tRNA–ACC (unpublished data), suggesting that under these conditions recognition of the very 3′ end is less critical. At best, our results indicate that AMV RNA has some rudimentary tRNA-like features.

We have shown here that the 3′ UTR of AMV and ilarvirus RNAs can exist in two mutually exclusive conformations, each of which plays a separate role in the viral life cycle. This property is potentially shared by other members of the Bromoviridae family whose 3′ UTRs can also be folded into two discrete configurations (Ahlquist *et al.*, 1981). For BMV it has been observed that upon lowering of the $Mg^{2+}$ concentration the pseudoknot disappears and a small hairpin emerges at the 3′ end (Rietveld *et al.*, 1983). Whether the BMV CP also plays a role in this process is not known, but since bromovirus infection does not require CP in the inoculum, a host protein may have taken over this function. Switching between the two conformations could enable the virus to

switch, e.g. from translation to replication, a fundamental issue for any RNA virus. A pseudoknot may be optimally suited for such a conformational switch, which might explain its presence in tRNA-like structures of many plant viral RNAs.

## Materials and methods

### *Sequence comparison*

Alfamo- and ilar-virus RNA sequences were retrieved from GenBank. DDBJ/EMBL/GenBank accession Nos are: AMV, L00164 [strain Q (1)], L00161 [strain Q (3)], U12510 [strain NZ2 (3)], U12509 [strain NZ1 (3)], M59241 [strain YSMV (3)], X00819 [strain S (3)], AF015717 [strain 15/64 (3)], AF015716 [strain VRU (3)], K02703 [strain 425 Madison (3)], L00163 [strain 425 Leiden (1)], K02702 [strain 425 Leiden (2)], K03542 [strain 425 Leiden (3)]; ApMV-I, U15608 (3); ApMV-G, S78319 (3); AV-2, X86352 (3); CiLRV, U23715 (1), U17726 (2), U17390 (3); CVV, U17389 (3); LRMV, U17391 (3); PDV, U57648 (1), L28145 (3); PNRSV, S78312 [strain PV96 (3)], L38823 [strain PE5 (3)], Y07568 [strain PV32 (3)]; TSV, U80934 (1), U75538 (2), X00435 (3); CiLRV, U23715 (1), U17726 (2), U17390 (3); SpLV, U93192 (1), U93193 (2), U93194 (3); and HdMV, U35145 (3). The numbers in parentheses refer to one of the three genomic RNAs.

### *Structure probing*

Four-microgram samples of purified AMV RNA4 were preincubated in 225 µl reaction buffer for 1 min at 65°C, then for 10 min at 37°C and finally for 10 min at room temperature (~21°C) to equilibrate the structure. Subsequently, the samples were incubated with 0, 2.5 or 5.0 µl of a DMS solution (10% v/v in ethanol) for 30 min at room temperature in 70 mM HEPES–KOH pH 7.8, 10 mM $MgCl_2$, 270 mM KCl. Reactions were stopped by the addition of 25 µl of 3 M sodium acetate pH 5.2, 5 µl β-mercaptoethanol and 625 µl ethanol. After precipitation of the RNA, primer extension was performed as described by Schmidt *et al.* (1987), with a primer complementary to the terminal 21 nt of AMV RNA. The products were fractionated on 8% polyacrylamide gels containing 8 M urea.

### *Construction of mutant AMV cDNA3 clones*

Plasmids 3kA4, 3kC2, 3kGC2, 3kG3 and 3kGC3, which after transcription by T7 polymerase yielded mutant A4, C2, GC2, G3 and GC3 RNA3 transcripts, respectively, were constructed as follows. First a 5′ fragment was synthesized by PCR on plasmid 3kWT (van der Vossen *et al.*, 1994), using primers T7G (**AATTTAATACGACTCACTATA**GGGTACCCCATTAATTTGG, the T7 promoter sequence is shown in bold, the underlined sequence represents a *Kpn*I restriction site used for cloning purposes) and HP4REV (CATACCTTGACCTTAATCCACC), which is complementary to the 5′ half of stem d (Figure 1) and partially complementary to primers HP4A4, L4GG and L4GGG. 3′ fragments containing the desired mutations in loop d and/or stem–loop a were generated using the following primer pairs: for mutant A4, HP4A4 (GGATTAAGGTCAAGGTATGAAGTCCTATT**AAAA**GATAGGATCGAC, mutated bases are shown in bold) and BIO358 (CTACCTGCAGCATCCCTTAGGGGCATTC, containing a *Pst*I restriction site); for mutant G3, L4GGG (GGATTAAGGTCAAGGTATGAAGTCCTATTCGCT**GGG**GATAGGATCGAC) and BIO358; for mutant GC2, L4GG (GGATTAAGGTCAAGGTATGAAGTCCTATTCGC**GG**CTGATAGGATCGAC) and M1CC (CTACCTGCAGCAT**GG**CTTAG**CC**GCATTCATGCAG); and for mutant GC3, primers L4GGG and M1CCC (CTACCTGCAGCAT**GGG**TTA**CCC**GCATTCATGCAG). 5′ and 3′ fragments were subsequently used in a second PCR and amplified using primers T7G and BIO358. The resulting fragments were cloned *Kpn*I–*Pst*I in p3kWT and checked by DNA sequencing. Construction of plasmid 3kC3 has been described previously (Reusken *et al.*, 1997). After linearization with *Pst*I and blunting with T4 DNA polymerase, transcripts were synthesized using T7 RNA polymerase (see below).

### *Synthesis of mutant transcripts*

Transcripts corresponding to the 3′ UTR of AMV RNA3, and mutants thereof, were synthesized by *in vitro* transcription with T7 RNA polymerase (Milligan *et al.*, 1987). The wt and mutant templates were constructed by PCR on the corresponding wt and mutant plasmids using primer T7G in combination with the appropriate reverse primers as indicated below. For WT, plasmid 3kWT and primer WT2 (GCATCCCTTAGGGGCATTCAT); for mutant GC3, plasmid 3kGC3 and reverse primer 1-8 (GCAT**GGG**TTA**CCC**GCATTCAT); for mutant C3, plasmid 3kC3 and primer 1–8; for mutant 1-7, plasmid 3k1-7 (Reusken *et al.*, 1997) and primer 1-7 (GCATCCCTTA**CCC**); for mutant A4, plasmid 3kA4 and primer WT2; and for mutant DR, plasmid 3kWT and primer DicRev (CGAATAGGACTTCATACCTTGACCTTAATCCACCCAG) were used. After transcription, reactions were DNase treated and phenol extracted; the RNA was precipitated twice from ammonium acetate/isopropanol, dissolved in sterile water and quantified on ethidium bromide-stained agarose gels. All enzymes were purchased from Gibco-BRL, except for Vent DNA polymerase (New England Biolabs, MA); oligonucleotides were purchased from Eurogentec (Belgium).

### *Inoculation of tobacco plants and protoplasts*

P12 tobacco plants were inoculated manually with wt and mutant RNA3, three half-leaves per plant. Virus particles were isolated 6 days after inoculation from 1.5 g of leaf material and viral RNA was extracted from the purified particles as described before (Reusken *et al.*, 1997). P12 protoplasts were inoculated with wt and mutant RNA3 transcripts by the PEG method as described (van der Vossen *et al.*, 1994). Total RNA was extracted from protoplasts using Trizol reagent (Gibco-BRL) 20 h after inoculation. RNA was analysed by Northern blotting using a DIG-labelled probe that detects the 3′ UTR of RNA1–4.

### *Adenylation*

Adenylation was carried out at room temperature for 2 h in a 10 µl reaction mixture containing 50 mM Tris–HCl pH 8.0, 50 mM NaCl, 10 mM $MgCl_2$, 10 mM $MnCl_2$, 50 µM ATP, 50 µM CTP (optional), 0.1 µM [$^{32}$P]ATP (ICN, 3000 Ci/mmol), 4 µM RNA and 1 µg of CTP/ATP:tRNA nucleotidyl transferase from baker's yeast, essentially as described (van Belkum *et al.*, 1985). Products were analysed on denaturing polyacrylamide gels (8%). Repeating the reactions at 4°C for 16 h led to similar results.

### *In vitro replication assay*

*Nicotiana benthamiana* plants infected with AMV were used to purify the AMV RdRp as described previously (Quadt *et al.*, 1991). Such a preparation is highly specific and dependent on added AMV template RNAs for its activity. This enzyme was used to study minus-strand RNA synthesis on wt and mutant AMV transcripts by incorporation of [$^{32}$P]UTP followed by S1 nuclease treatment and separation of the products on agarose gels, all as described previously (de Graaff *et al.*, 1995). To study the effect of added CP on minus-strand synthesis RNAs (20 pmol) corresponding to the 3′ UTR of wt or mutant 1-7, RNA3 were pre-incubated with CP (0–40 pmol) at room temperature in 3 µl containing 33 mM NaOAc pH 6.0, 13% Tween-20 and 13% glycerol for 15 min. Subsequently, the RdRp reaction mixture (22 µl) was added and incubation continued for 30 min at 28°C. Reactions were stopped by the addition of formamide loading buffer and directly electrophoresed in a 6% polyacrylamide gel.

### *Band shift assay*

$^{32}$P-labelled transcripts D/WT and D/A4 were synthesized by *in vitro* transcription in the presence of [$^{32}$P]UTP. Templates were obtained by PCR using primers T7D (**AATTTAATACGACTCACTATA**GGGTATGAAGTCCTATTCG) and WT2 on plasmids 3kWT and 3kA4, respectively. Due to mispriming of primer T7D on 3kA4 the d-loop sequence becomes CGAA instead of AAAA; this has no consequences for this experiment. Conditions for the band shift assay were as follows. One microgram (~20 pmol) of labelled transcript was preheated for 2 min at 65°C in a buffer containing 75 mM Tris–HCl pH 8.0 (+15 mM $MgCl_2$ for assays in the presence of $Mg^{2+}$) and then slowly cooled to room temperature. One microgram (~8 pmol) of yeast tRNA and 5 pmol of CP were added and the reactions were brought to 50 mM Tris–HCl pH 8.0 (+10 mM $MgCl_2$ for assays in the presence of $Mg^{2+}$). After 15 min of incubation at room temperature, glycerol loading buffer was added and samples were electrophoresed in a 6% polyacrylamide gel. The gel was dried and exposed to X-ray film.

## Acknowledgements

We thank Dr C.W.A.Pleij for fruitful discussions, P.W.G.Verlaan for his gift of CTP/ATP tRNA nucleotidyl transferase and Dr R.Miglino for performing protoplast experiments and photographic work.

## References


Ahlquist,P., Dasgupta,R. and Kaesberg,P. (1981) Near identity of 3′ RNA secondary structure in bromoviruses and cucumber mosaic virus. *Cell*, **23**, 183–189.

Ansel-McKinney,P. and Gehrke,L. (1998) RNA determinants of a specific RNA–coat protein peptide interaction in alfalfa mosaic virus: conservation of homologous features in ilarvirus RNAs. *J. Mol. Biol.*, **278**, 767–785.

Asano,K. and Mizobuchi,K. (1998) Copy number control of *Inc*Iα plasmid *Col*Ib–P9 by competition between pseudoknot formation and antisense RNA binding at a specific RNA site. *EMBO J.*, **17**, 5201–5213.

Baer,M., Houser,F., Loesch-Fries,L.S. and Gehrke,L. (1994) Specific RNA binding by N-terminal peptides of alfalfa mosaic virus coat protein. *EMBO J.*, **13**, 727–735.

Bol,J.F. (1999) Alfalfa mosaic virus and ilarviruses: involvement of coat protein in multiple steps of the replication cycle. *J. Gen. Virol.*, **80**, 1089–1102.

Chapman,M.R. and Kao,C.C. (1999) A minimal RNA promoter for minus-strand RNA synthesis by the brome mosaic virus polymerase complex. *J. Mol. Biol.*, **286**, 709–720.

de Graaff,M., Coscoy,L. and Jaspars,E.M.J. (1993) Localization and biochemical characterization of alfalfa mosaic virus replication complexes. *Virology*, **194**, 878–881.

de Graaff,M., Man in 't Veld,M.R. and Jaspars,E.M.J. (1995) *In vitro* evidence that the coat protein of alfalfa mosaic virus plays a direct role in regulation of plus and minus RNA synthesis: implications for the life cycle of alfalfa mosaic virus. *Virology*, **208**, 583–589.

Deiman,B.A.L.M. (1999) Initiation of turnip yellow mosaic virus RNA replication by the viral polymerase. PhD thesis, Leiden University, The Netherlands.

Deiman,B.A.L.M., Koenen,A.K., Verlaan,P.W.G. and Pleij,C.W.A. (1998) Minimal template requirements for initiation of minus-strand synthesis *in vitro* by the RNA-dependent RNA polymerase of turnip yellow mosaic virus. *J. Virol.*, **72**, 3965–3972.

Draper,D.E. (1996) Strategies for RNA folding. *Trends Biochem. Sci.*, **21**, 145–149.

Dreher,T.W. and Hall,T.C. (1988) Mutational analysis of the sequence and structural requirements in brome mosaic virus RNA for minus-strand promoter activity. *J. Mol. Biol.*, **201**, 31–40.

Dreher,T.W., Rao,A.L.N. and Hall,T.C. (1989) Replication *in vivo* of mutant brome mosaic virus RNAs defective in aminoacylation. *J. Mol. Biol.*, **206**, 425–438.

Felden,B., Florentz,C., Westhof,E. and Giegé,R. (1998) Transfer RNA identity rules and conformation of the tyrosine tRNA-like domain of BMV RNA imply additional charging by histidine and valine. *Biochem. Biophys. Res. Commun.*, **243**, 426–434.

Giegé,R. (1996) Interplay of tRNA-like structures from plant viral RNAs with partners of the translation and replication machineries. *Proc. Natl Acad. Sci. USA*, **93**, 12078–12081.

Gluick,T.C., Wills,N.M., Gesteland,R. and Draper,D.E. (1997) Folding of an mRNA pseudoknot required for stop codon readthrough: effects of mono- and di-valent cations on stability. *Biochemistry*, **36**, 16173–16186.

Goodwin,J.B. and Dreher,T.W. (1998) Transfer RNA mimicry in a new group of positive-strand RNA plant viruses, the furoviruses: differential aminoacylation between the RNA components of one genome. *Virology*, **246**, 170–178.

Goodwin,J.B., Skuzeski,J.M. and Dreher,T.W. (1997) Characterization of chimeric turnip yellow mosaic virus genomes that are infectious in the absence of aminoacylation. *Virology*, **230**, 113–124.

Grieco,F., Dell'Orco,M. and Martelli,G.P. (1996) The nucleotide sequence of RNA 1 and RNA 2 of olive latent virus 2 and its relationships in the family *Bromoviridae*. *J. Gen. Virol.*, **77**, 2637–2644.

Haenni,A.-L. and Chapeville,F. (1997) An enigma: the role of viral RNA aminoacylation. *Acta Biochim. Pol.*, **44**, 827–838.

Hall,T.C. (1979) Transfer RNA-like structures in viral genomes. *Int. Rev. Cytol.*, **60**, 1–26.

Hann,L.E., Webb,A.C., Cai,J.-M. and Gehrke,L. (1997) Identification of a competitive translation determinant in the 3′ untranslated region of alfalfa mosaic virus coat protein mRNA. *Mol. Cell. Biol.*, **17**, 2005–2013.

Hinz,H.-J., Srinivasan,S. and Jaspars,E.M.J. (1979) Energetics of the thermal transitions of RNA1 and RNA4 of alfalfa mosaic virus in the presence and absence of coat protein. *Eur. J. Biochem.*, **95**, 107–114.

Houser-Scott,F., Ansel-McKinney,P., Cai,J.-M. and Gehrke,L. (1997) *In vitro* genetic selection analysis of alfalfa mosaic virus coat protein binding to 3′-terminal AUGC repeats in the viral RNAs. *J. Virol.*, **71**, 2310–2319.

Houwing,C.J. and Jaspars,E.M.J. (1982) Protein binding sites in nucleation complexes of alfalfa mosaic virus RNA 4. *Biochemistry*, **21**, 3408–3414.

Jaspars,E.M.J. (1999) Genome activation in alfamo- and ilar-viruses. *Arch. Virol.*, **144**, 843–863.

Kolk,M.H., van der Graaf,M., Wijnenga,S.S., Pleij,C.W.A., Heus,H.A. and Hilbers,C.W. (1998) NMR structure of a classical pseudoknot. Interplay of single- and double-stranded RNA. *Science*, **280**, 434–438.

Koper-Zwarthoff,E.C. and Bol,J.F. (1980) Nucleotide sequence of the putative recognition site for coat protein in the RNAs of alfalfa mosaic virus and tobacco streak virus. *Nucleic Acids Res.*, **8**, 3307–3318.

Koper-Zwarthoff,E.C., Brederode,F.T., Walstra,P. and Bol,J.F. (1979) Nucleotide sequence of the 3′-noncoding region of alfalfa mosaic virus RNA 4 and its homology with the genomic RNAs. *Nucleic Acids Res.*, **7**, 1887–1900.

Kozlov,Y.V., Rupasov,V.V., Adyshev,D.M., Belgelarskaya,S.N., Agranovsky,A.A., Mankin,A.S., Morozov,S.Y., Dolja,V.V. and Atabekov,J.G. (1984) Nucleotide sequence of the 3′-terminal tRNA-like structure in barley stripe mosaic virus genome. *Nucleic Acids Res.*, **12**, 4001–4009.

Lahser,F.C., Marsh,L.E. and Hall,T.C. (1993) Contributions of the brome mosaic virus RNA-3 3′-nontranslated region to replication and translation. *J. Virol.*, **67**, 3295–3303.

Leathers,V., Tanguay,R., Kobayashi,M. and Gallie,D.R. (1993) A phylogenetically conserved sequence within viral 3′ untranslated RNA pseudoknots regulates translation. *Mol. Cell. Biol.*, **13**, 5331–5347.

Mans,R.M.W., Pleij,C.W.A. and Bosch,L. (1991) tRNA-like structures. Structure, function and evolutionary significance. *Eur. J. Biochem.*, **201**, 303–324.

Mans,R.M.W., van Steeg,M.H., Verlaan,P.W.G., Pleij,C.W.A. and Bosch,L. (1992) Mutational analysis of the pseudoknot in the tRNA-like structure of turnip yellow mosaic virus RNA: aminoacylation efficiency and pseudoknot stability. *J. Mol. Biol.*, **223**, 221–232.

Milligan,J.F., Groebe,D.R., Witherell,G.W. and Uhlenbeck,O.C. (1987) Oligonucleotide synthesis using T7 RNA polymerase and synthetic DNA templates. *Nucleic Acids Res.*, **15**, 8783–8798.

Neeleman,L., van der Vossen,E.A.G. and Bol,J.F. (1993) Infection of tobacco with alfalfa mosaic virus cDNAs sheds light on the early function of the coat protein. *Virology*, **196**, 883–887.

Pleij,C.W.A. (1994) Pseudoknots. *Curr. Opin. Struct. Biol.*, **4**, 337–344.

Pringle,C.R. (1998) The universal system of virus taxonomy of the International Committee on Virus Taxonomy (ICTV), including new proposals ratified since publication of the sixth ICTV report in 1995. *Arch. Virol.*, **143**, 203–210.

Quadt,R., Rosdorff,H.J.M., Hunt,T.W. and Jaspars,E.M.J. (1991) Analysis of the protein composition of alfalfa mosaic virus RNA-dependent RNA polymerase. *Virology*, **182**, 309–315.

Quigley,G.J., Gehrke,L., Roth,D.A. and Auron,P.E. (1984) Computer-aided nucleic acid secondary structure modeling incorporating enzymatic digestion data. *Nucleic Acids Res.*, **12**, 347–366.

Reusken,C.B.E.M. and Bol,J.F. (1996) Structural elements of the 3′-terminal coat protein binding site in alfalfa mosaic virus RNAs. *Nucleic Acids Res.*, **24**, 2660–2665.

Reusken,C.B.E.M., Neeleman,L., Brederode,F.T. and Bol,J.F. (1997) Mutations in coat protein binding sites of alfalfa mosaic virus RNA 3 affect subgenomic RNA 4 accumulation and encapsidation of viral RNAs. *J. Virol.*, **71**, 8385–8391.

Rietveld,K., Pleij,C.W.A. and Bosch,L. (1983) Three-dimensional models of the tRNA-like 3′ termini of some plant viral RNAs. *EMBO J.*, **2**, 1079–1085.

Ryabova,L.A., Torgashov,A.F., Kurnasov,O.V., Bubunenko,M.G. and Spirin,A.S. (1993) The 3′-terminal untranslated region of alfalfa mosaic virus RNA-4 facilitates the RNA entry into translation in a cell-free system. *FEBS Lett.*, **326**, 264–266.

Schmidt,B.F., Berkhout,B., Overbeek,G.P., van Strien,A. and van Duin,J. (1987) Determination of the RNA secondary structure that regulates lysis gene expression in bacteriophage MS2. *J. Mol. Biol.*, **195**, 505–516.

Shi,P.-Y., Weiner,A.M. and Maizels,N. (1998) A top-half tDNA minihelix is a good substrate for the eubacterial CCA-adding enzyme. *RNA*, **4**, 276–284.

Singh,R.N. and Dreher,T.W. (1998) Specific site selection in RNA resulting from the combination of nonspecific secondary structure and –CCR– boxes: initiation of minus-strand synthesis by turnip

yellow mosaic virus RNA-dependent RNA polymerase. *RNA*, **4**, 1083–1095.
Skuzeski,J.M., Bozarth,C.S. and Dreher,T.W. (1996) The turnip yellow mosaic virus tRNA-like structure cannot be replaced by generic tRNA-like elements or by heterologous 3′ untranslated regions known to enhance mRNA expression and stability. *J. Virol.*, **70**, 2107–2115.
Srinivasan,S. and Jaspars,E.M.J. (1978) Influence of a few coat protein subunits on the base-paired structure of the RNA species of alfalfa mosaic virus. *Biochim. Biophys. Acta*, **520**, 237–241.
Srinivasan,S. and Jaspars,E.M.J. (1979) Influence of a few coat protein subunits on the base-paired structure of 3′-terminal fragments of RNA4 of alfalfa mosaic virus. *Biochim. Biophys. Acta*, **561**, 535–539.
Srinivasan,S. and Jaspars,E.M.J. (1982) Alterations of the conformation of the RNAs of alfalfa mosaic virus upon binding of a few coat protein molecules. *Biochim. Biophys. Acta*, **696**, 260–266.
Taschner,P.E.M., van der Kuyl,A.C., Neeleman,L. and Bol,J.F. (1991) Replication of an incomplete alfalfa mosaic virus genome in plants transformed with viral replicase genes. *Virology*, **181**, 445–450.
van Belkum,A., Abrahams,J.P., Pleij,C.W.A. and Bosch,L. (1985) Five pseudoknots are present at the 204 nucleotides long 3′-noncoding region of tobacco mosaic virus RNA. *Nucleic Acids Res.*, **13**, 7673–7686.
van der Vossen,E.A.G., Neeleman,L. and Bol,J.F. (1994) Early and late functions of alfalfa mosaic virus coat protein can be mutated separately. *Virology*, **202**, 891–903.
Wyatt,J.R., Puglisi,J.D. and Tinoco,I.,Jr. (1990) RNA pseudoknots. Stability and loop size requirements. *J. Mol. Biol.*, **214**, 455–470.
Zuidema,D (1983) Specific binding sites on RNAs and coat protein of alfalfa mosaic virus involved in genome activation. PhD thesis, Leiden University, The Netherlands.

*Received May 19, 1999; revised and accepted July 17, 1999*